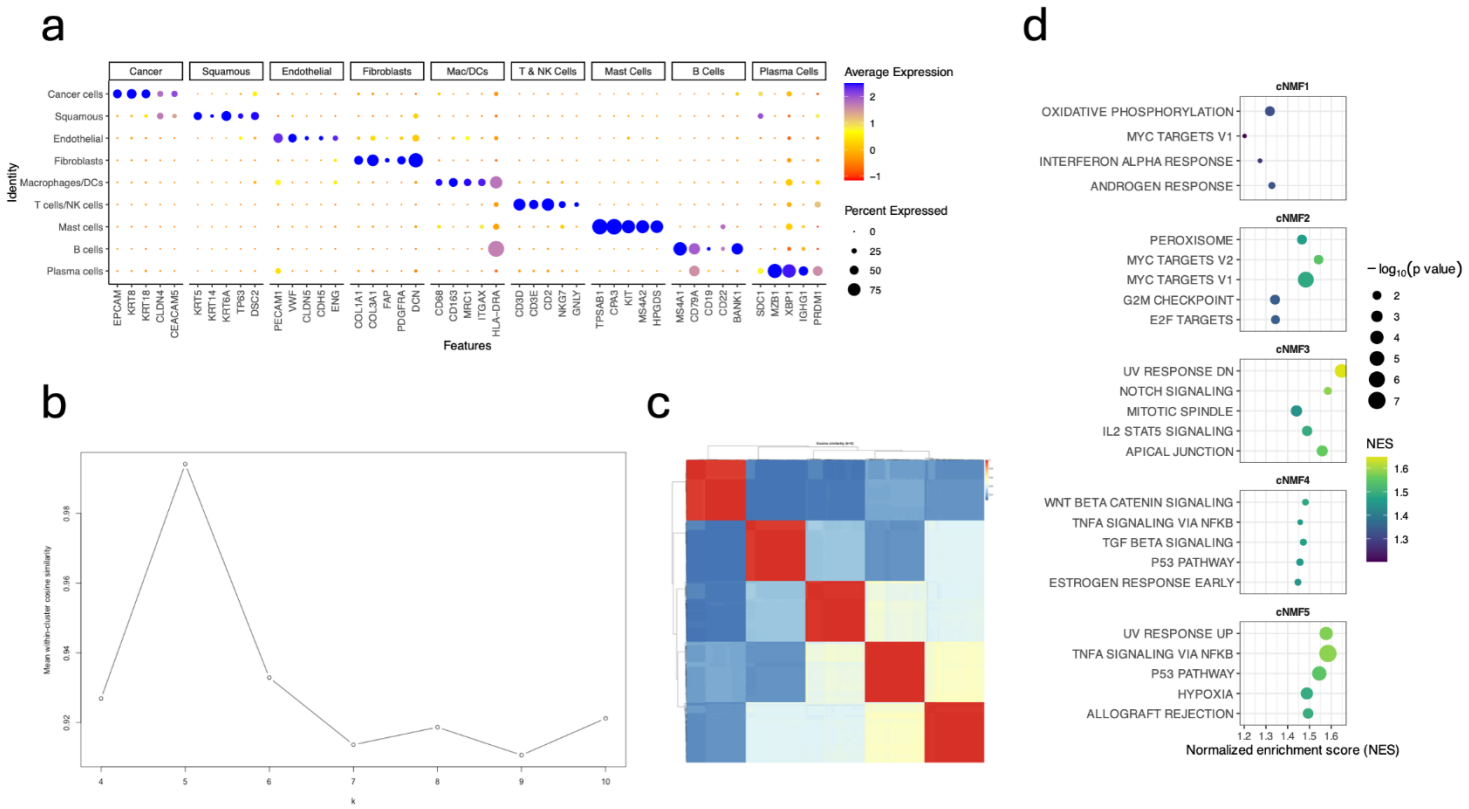
a
Cancer
Squamous
Endothelial
Fibroblasts
Mac/DCs
T & NK Cells
Mast Cells
B Cells
Plasma Cells
Identity
Cancer cells
Squamous
Endothelial
Fibroblasts
Macrophages/DCs
T cells/NK cells
Mast cells
B cells
Plasma cells
EPCAM KRT8 KRT18 CLDN4 CEACAM5
KRT5 KRT14 KRT6A TP63 DSC2
PECAM1 VWF CLDN5 CDH5 ENG
COL1A1 COL3A1 FAP PDGFRA DCN
CD68 CD163 MRC1 ITGAX HLA-DRA
CD3D CD3E CD2 NKG7 GNLY
TPSAB1 CPA3 KIT MS4A2 HPGDS
MS4A1 CD79A CD19 CD22 BANK1
SDC1 MZB1 XBP1 IGHG1 PRDM1
Features
Average Expression
2
1
0
−1
Percent Expressed
0
25
50
75
b
Mean within-cluster cosine similarity
0.92
0.94
0.96
0.98
4
5
6
7
8
9
10
k
c
d
cNMF1
OXIDATIVE PHOSPHORYLATION
MYC TARGETS V1
INTERFERON ALPHA RESPONSE
ANDROGEN RESPONSE
cNMF2
PEROXISOME
MYC TARGETS V2
MYC TARGETS V1
G2M CHECKPOINT
E2F TARGETS
cNMF3
UV RESPONSE DN
NOTCH SIGNALING
MITOTIC SPINDLE
IL2 STAT5 SIGNALING
APICAL JUNCTION
cNMF4
WNT BETA CATENIN SIGNALING
TNFA SIGNALING VIA NFKB
TGF BETA SIGNALING
P53 PATHWAY
ESTROGEN RESPONSE EARLY
cNMF5
UV RESPONSE UP
TNFA SIGNALING VIA NFKB
P53 PATHWAY
HYPOXIA
ALLOGRAFT REJECTION
1.2 1.3 1.4 1.5 1.6
Normalized enrichment score (NES)
−log10(p value)
2
3
4
5
6
7
NES
1.6
1.5
1.4
1.3

Supplementary Figure S1 Integrated single-cell reference and derivation of malignant transcriptional programmes. a) Dot plot showing canonical marker-gene expression across broad cell lineages in the single-cell RNA-seq reference. Dot size indicates the percentage of cells expressing each marker and colour indicates scaled average expression. **b)** Stability assessment of consensus NMF solutions across candidate ranks, shown as mean within-cluster cosine similarity. **c)** Pairwise cosine similarity heatmap of the five consensus malignant transcriptional programmes selected for downstream analysis. **d)** Hallmark pathway enrichment of cNMF programmes, with point position showing normalised enrichment score and point size indicating statistical significance.

BIOPSY

RESECTION

OAC1

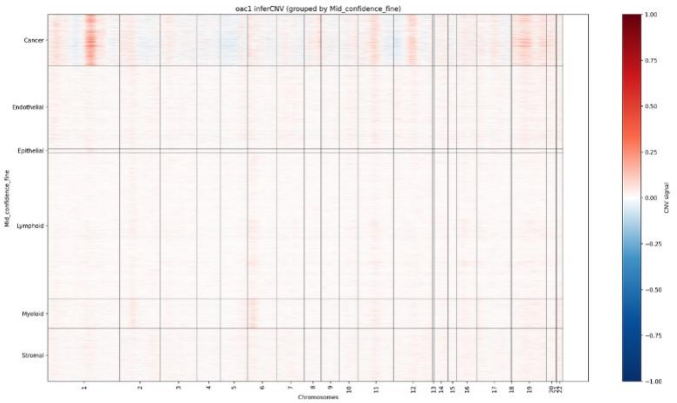

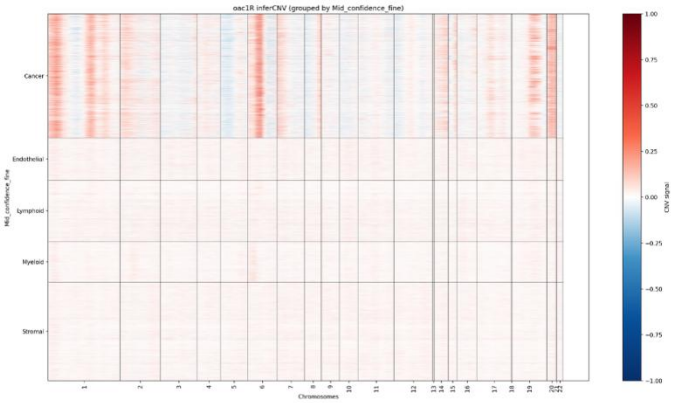

OAC2

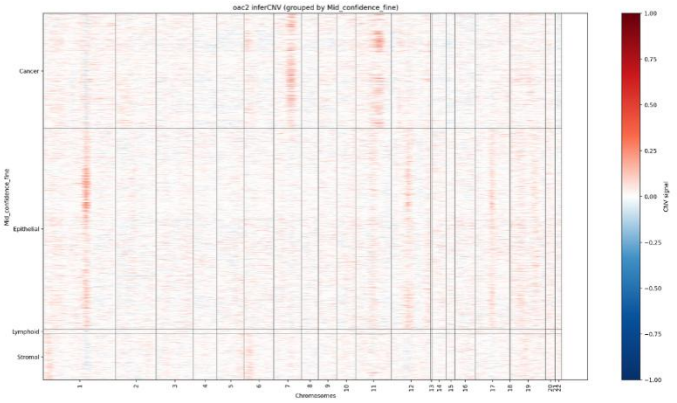

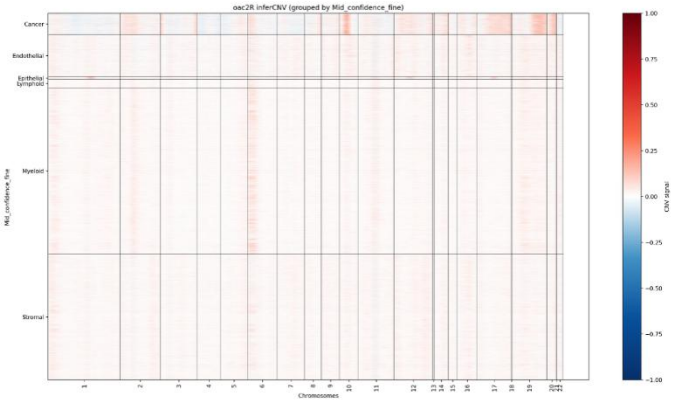

OAC3

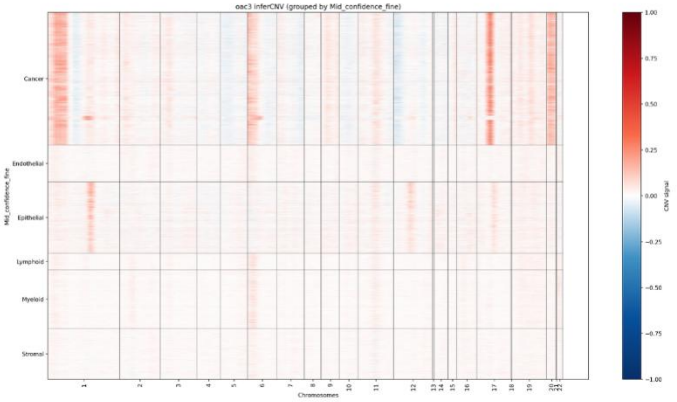

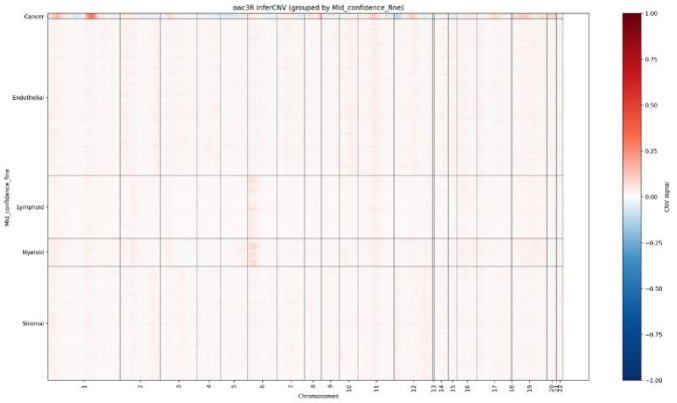

OAC4

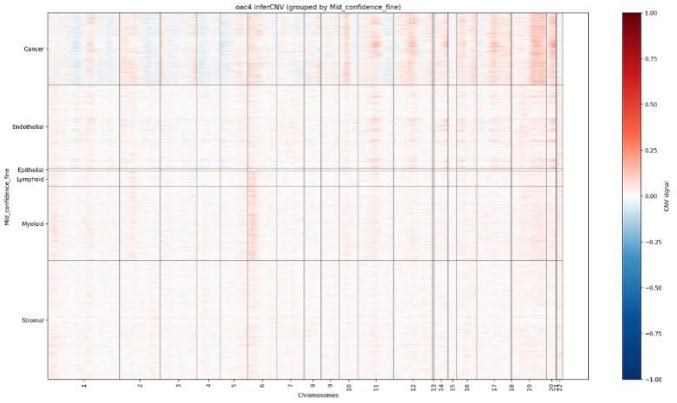

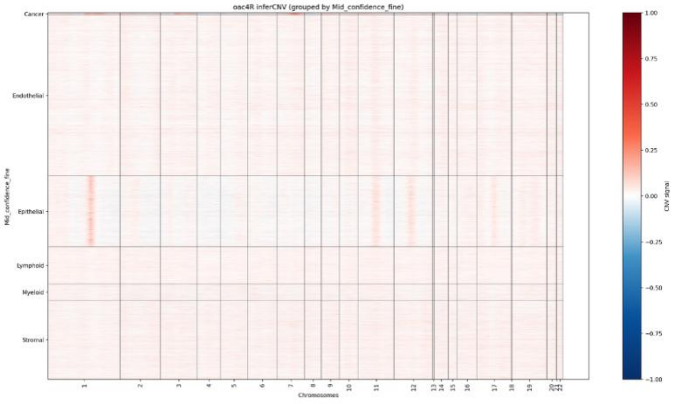

OAC5

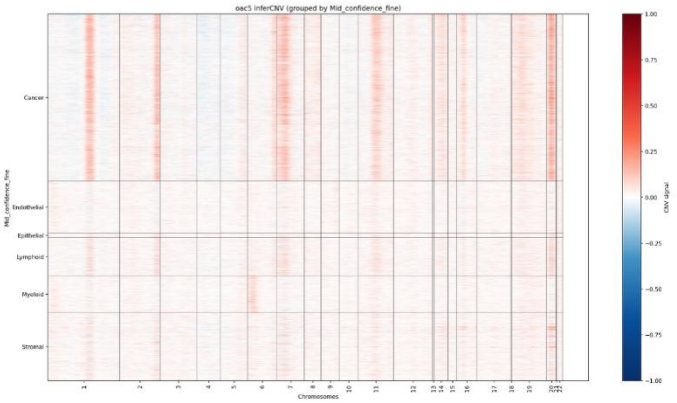

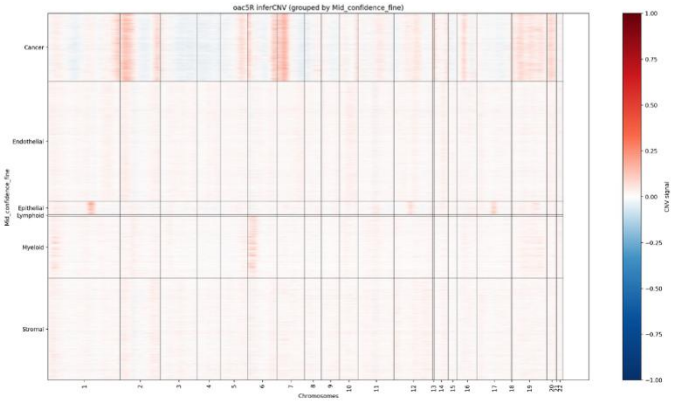

Supplementary Figure S2 Expression-derived copy-number alteration signal in paired biopsy and resection CosMx samples. infercnvpy heatmaps showing putative large-scale copy-number alteration-like signal inferred from CosMx expression data for paired biopsy and post-treatment resection samples from five OAC cases. Cells are grouped by refined cell annotation and genes are ordered by genomic position across autosomes. Red and blue indicate relative inferred gains and losses, respectively, compared with non-malignant reference populations. These profiles represent transcriptome-derived CNA-like signal and not direct DNA copy-number calls.

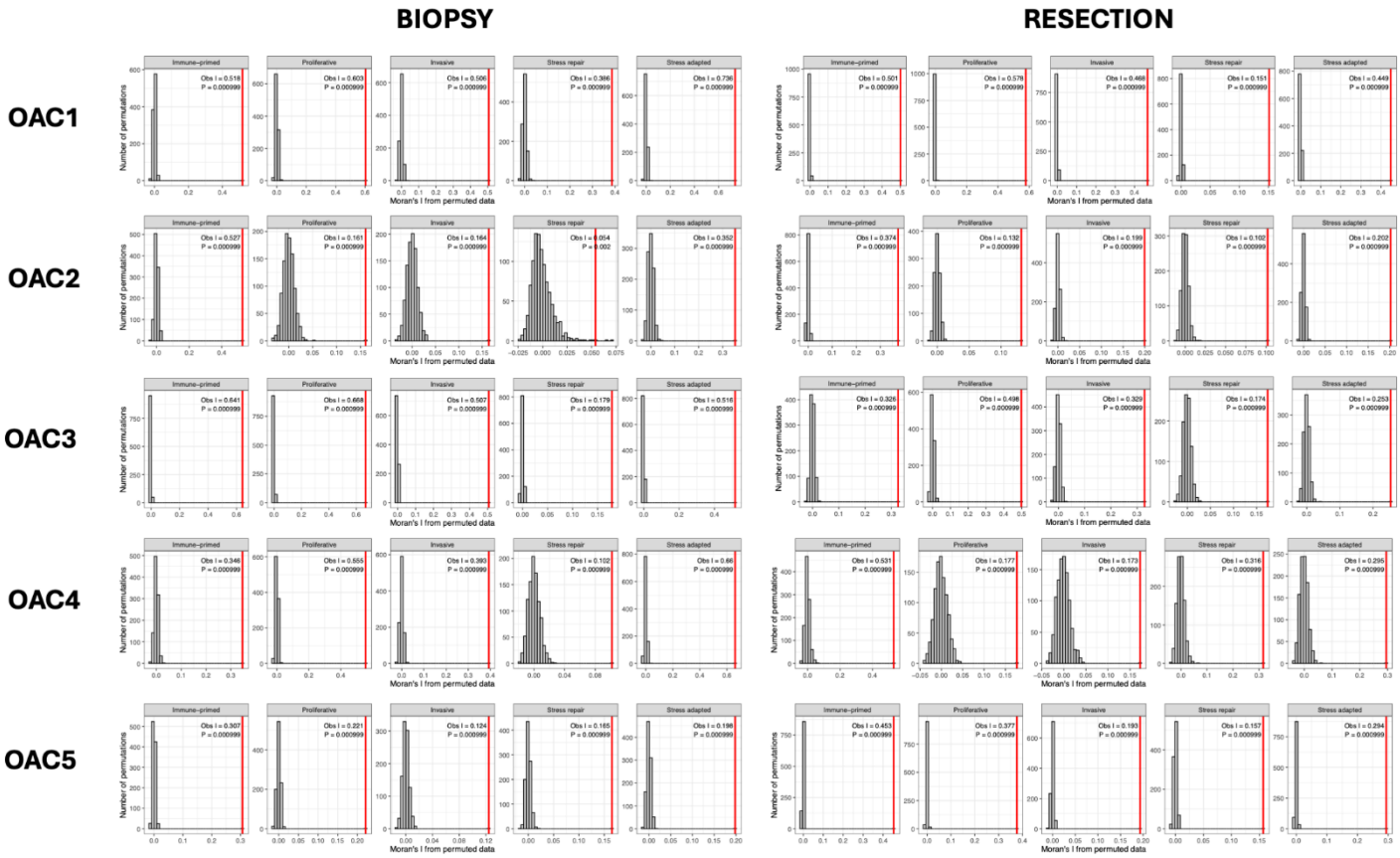
BIOPSY
RESECTION
OAC1
OAC2
OAC3
OAC4
OAC5
Immune−primed
Proliferative
Invasive
Stress repair
Stress adapted
Number of permutations
Moran's I from permuted data

Supplementary Figure S3 Permutation testing of spatial autocorrelation for malignant transcriptional programmes. Histograms show the permutation-derived null distribution of Moran's I for each cNMF tumour programme in biopsy and resection samples from OAC1–OAC5. Continuous programme scores were analysed across cancer-cell spatial neighbour graphs. Red vertical lines indicate the observed Moran's I statistic, with observed values and permutation P values shown within each panel. Positive observed Moran's I values indicate spatial clustering of malignant programme activity.

a

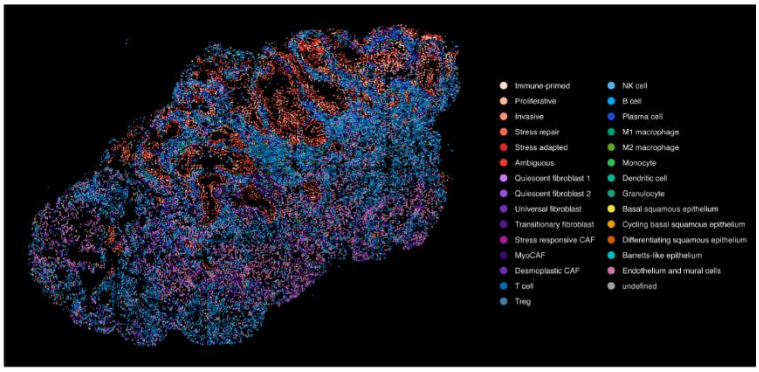
Immune-primed
Proliferative
Invasive
Stress repair
Stress adapted
Ambiguous
Quiescent fibroblast 1
Quiescent fibroblast 2
Universal fibroblast
Transitionary fibroblast
Stress responsive CAF
MyoCAF
Desmoplastic CAF
T cell
Treg
NK cell
B cell
Plasma cell
M1 macrophage
M2 macrophage
Monocyte
Dendritic cell
Granulocyte
Basal squamous epithelium
Cycling basal squamous epithelium
Differentiating squamous epithelium
Barretts-like epithelium
Endothelium and mural cells
undefined

b

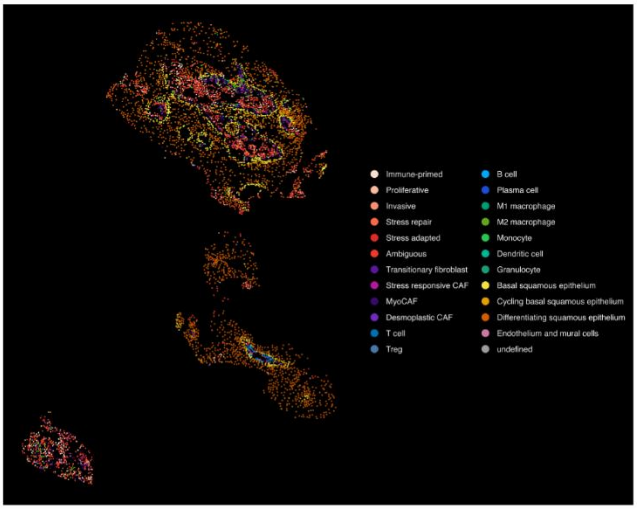
Immune-primed
Proliferative
Invasive
Stress repair
Stress adapted
Ambiguous
Transitionary fibroblast
Stress responsive CAF
MyoCAF
Desmoplastic CAF
T cell
Treg
B cell
Plasma cell
M1 macrophage
M2 macrophage
Monocyte
Dendritic cell
Granulocyte
Basal squamous epithelium
Cycling basal squamous epithelium
Differentiating squamous epithelium
Endothelium and mural cells
undefined

c

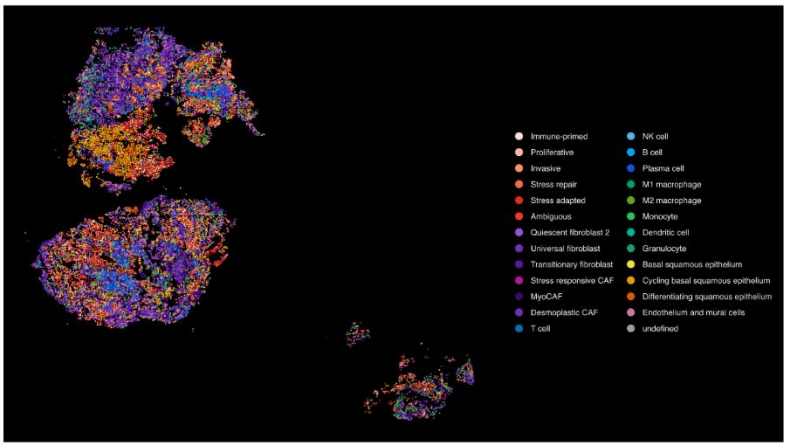
Immune-primed
Proliferative
Invasive
Stress repair
Stress adapted
Ambiguous
Quiescent fibroblast 2
Universal fibroblast
Transitionary fibroblast
Stress responsive CAF
MyoCAF
Desmoplastic CAF
T cell
NK cell
B cell
Plasma cell
M1 macrophage
M2 macrophage
Monocyte
Dendritic cell
Granulocyte
Basal squamous epithelium
Cycling basal squamous epithelium
Differentiating squamous epithelium
Endothelium and mural cells
undefined

d

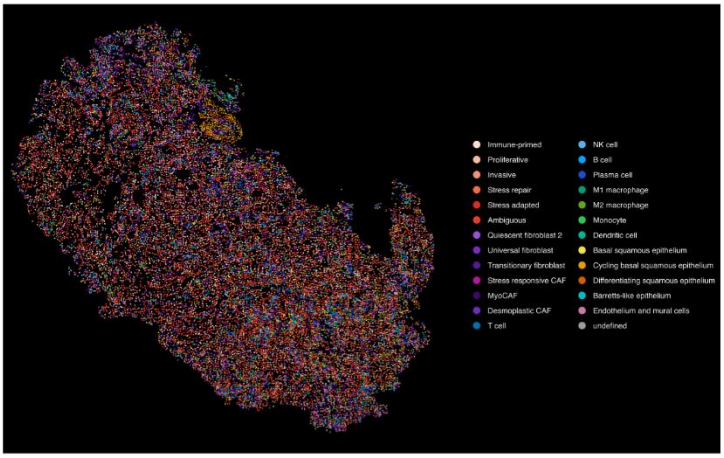
Immune-primed
Proliferative
Invasive
Stress repair
Stress adapted
Ambiguous
Quiescent fibroblast 2
Universal fibroblast
Transitionary fibroblast
Stress responsive CAF
MyoCAF
Desmoplastic CAF
T cell
NK cell
B cell
Plasma cell
M1 macrophage
M2 macrophage
Monocyte
Dendritic cell
Basal squamous epithelium
Cycling basal squamous epithelium
Differentiating squamous epithelium
Barretts-like epithelium
Endothelium and mural cells
undefined

e

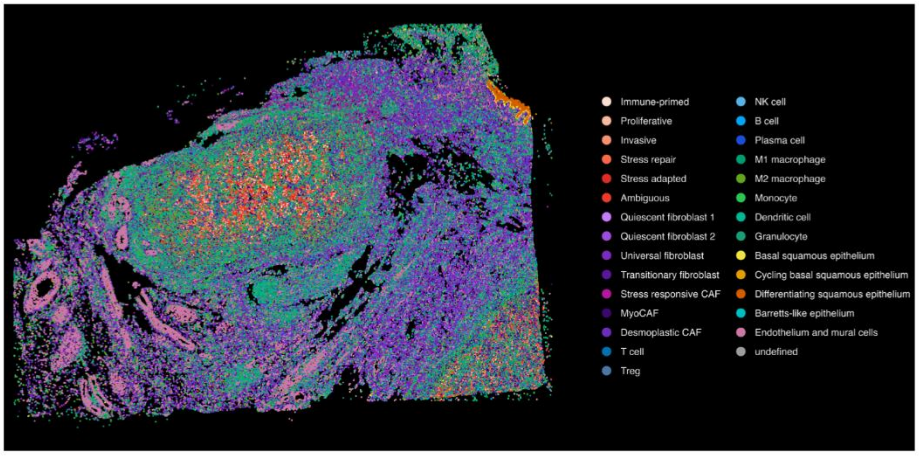
Immune-primed
Proliferative
Invasive
Stress repair
Stress adapted
Ambiguous
Quiescent fibroblast 1
Quiescent fibroblast 2
Universal fibroblast
Transitionary fibroblast
Stress responsive CAF
MyoCAF
Desmoplastic CAF
T cell
Treg
NK cell
B cell
Plasma cell
M1 macrophage
M2 macrophage
Monocyte
Dendritic cell
Granulocyte
Basal squamous epithelium
Cycling basal squamous epithelium
Differentiating squamous epithelium
Barretts-like epithelium
Endothelium and mural cells
undefined

f

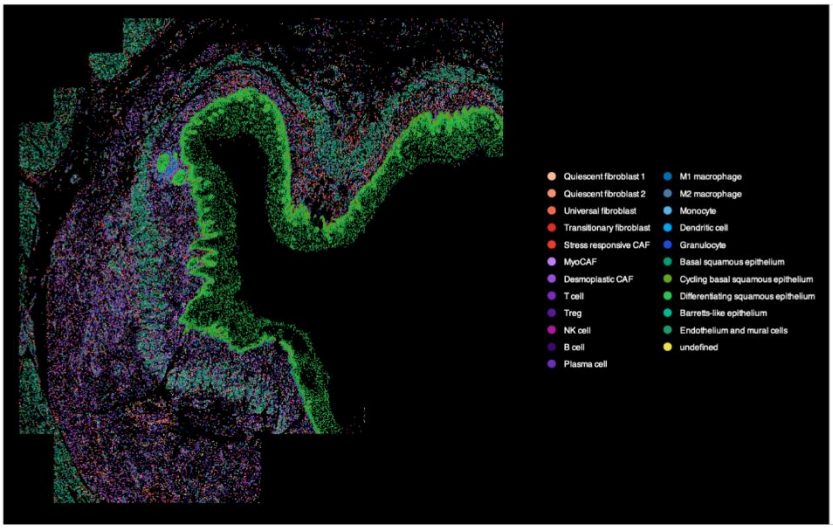
Quiescent fibroblast 1
Quiescent fibroblast 2
Universal fibroblast
Transitionary fibroblast
Stress responsive CAF
MyoCAF
Desmoplastic CAF
T cell
Treg
NK cell
B cell
Plasma cell
M1 macrophage
M2 macrophage
Monocyte
Dendritic cell
Granulocyte
Basal squamous epithelium
Cycling basal squamous epithelium
Differentiating squamous epithelium
Barretts-like epithelium
Endothelium and mural cells
undefined

Supplementary Figure S4 Spatial mapping of final CosMx cell-type and cancer-programme annotations. Representative CosMx tissue sections showing cell centroid maps coloured by final refined annotation. Labels include malignant cNMF programmes, epithelial states, fibroblast/CAF states, endothelial and mural cells, and immune populations. Spatial maps illustrate the tissue distribution of annotated cell types and malignant transcriptional states across profiled sections.

OAC1

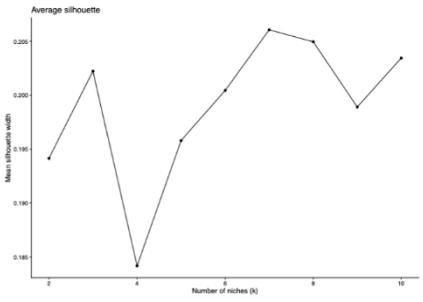

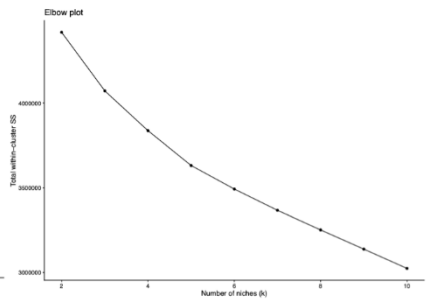

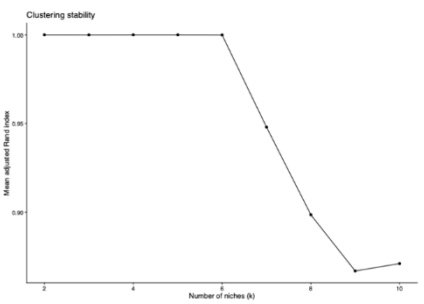

OAC2

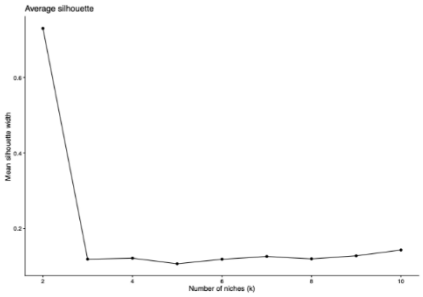

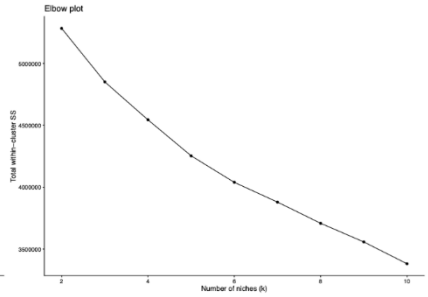

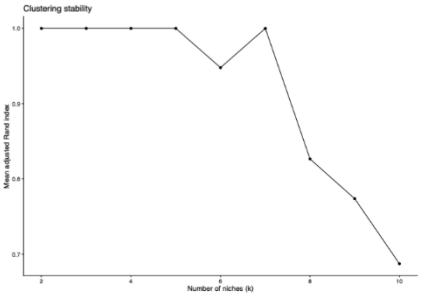

OAC3

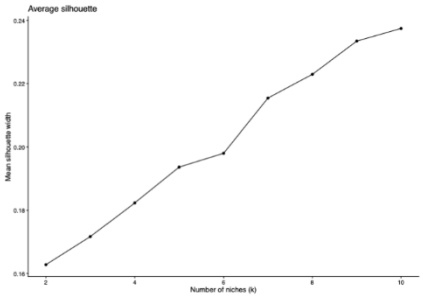

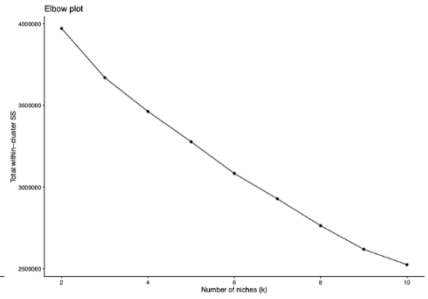

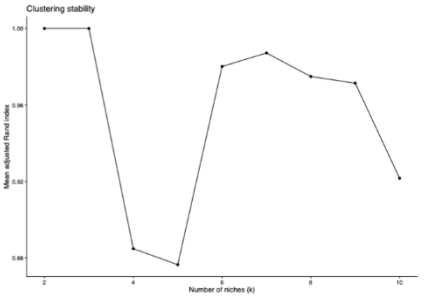

OAC4

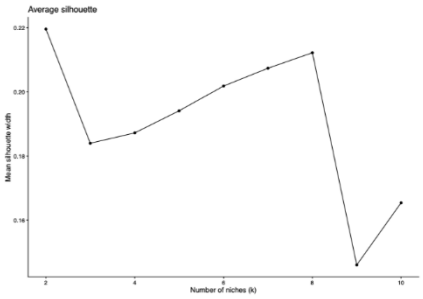

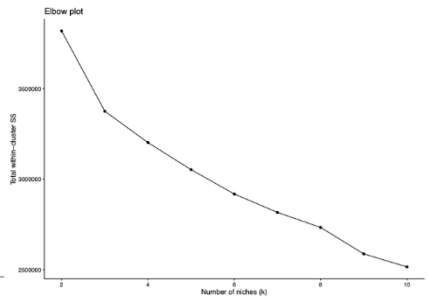

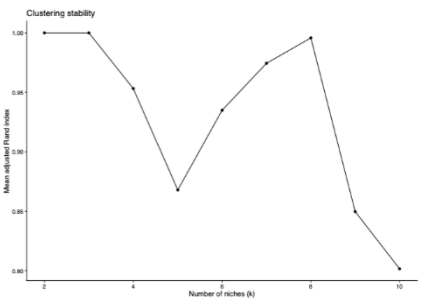

OAC5

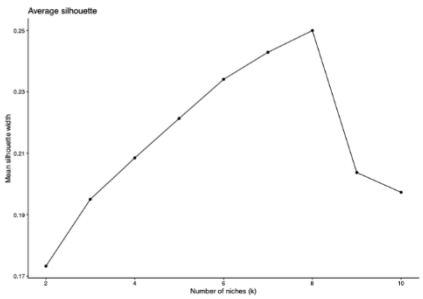

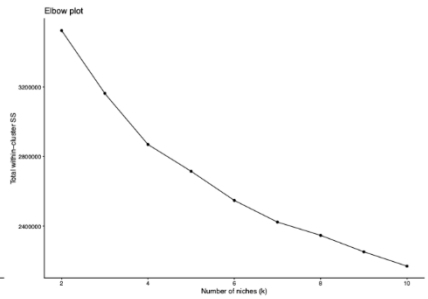

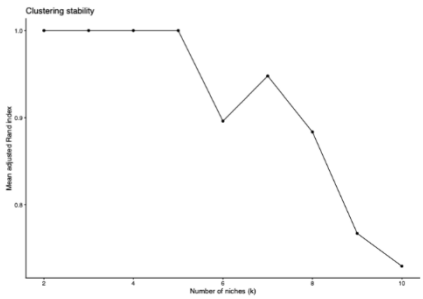

Supplementary Figure S5 Selection of spatial niche cluster number. Sample-level metrics used to select the number of unsupervised spatial niches in each resection sample. For OAC1–OAC5, candidate niche numbers were evaluated using average silhouette width, total within-cluster sum of squares, and clustering stability measured by mean adjusted Rand index. Final niche numbers were selected by balancing separation, stability, parsimony, and biological interpretability.

a

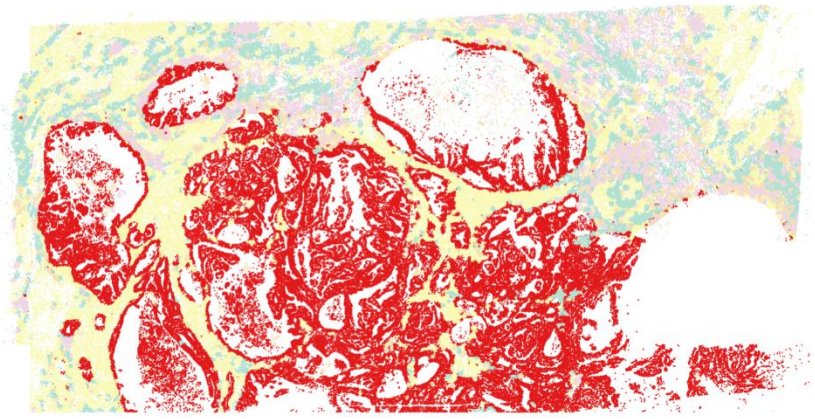

OAC1R

Niche 1
Quiescent fib 1, Quiescent fib 2, Univ. fib, Trans. fib, Stress CAF, DesmoCAF

Niche 2
Cancer, Trans. fib, MyoCAF, M2 Mac, DC

Niche 3
Quiescent fib 2, B cell, Plasma, M1 Mac, Mono, DC, Gran, Endo/mural

Niche 4
Quiescent fib 1, Quiescent fib 2, T cell, Treg, B cell, Plasma, M1 Mac, DC

Niche 5
Quiescent fib 1, Quiescent fib 2, T cell, Treg, NK cell, B cell, Plasma, M1 Mac

b

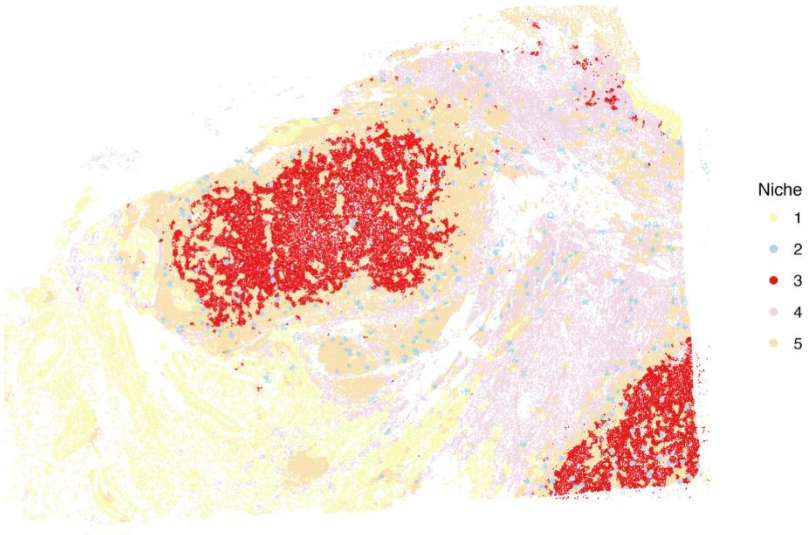

OAC2R

Niche 1
Quiescent fib 1, Univ. fib, Trans. fib, Basal squam. epi, Cycling basal squam. epi, Diff. squam, epi, Barrett's-like epi, Endo/mural

Niche 2
T cell, Treg, NK cell, B cell, Plasma

Niche 3
Cancer, MyoCAF, M2 Mac

Niche 4
Quiescent fib 1, Quiescent fib 2, DesmoCAF

Niche 5
T cell, NK cell, B cell, Plasma, DC, Gran

c

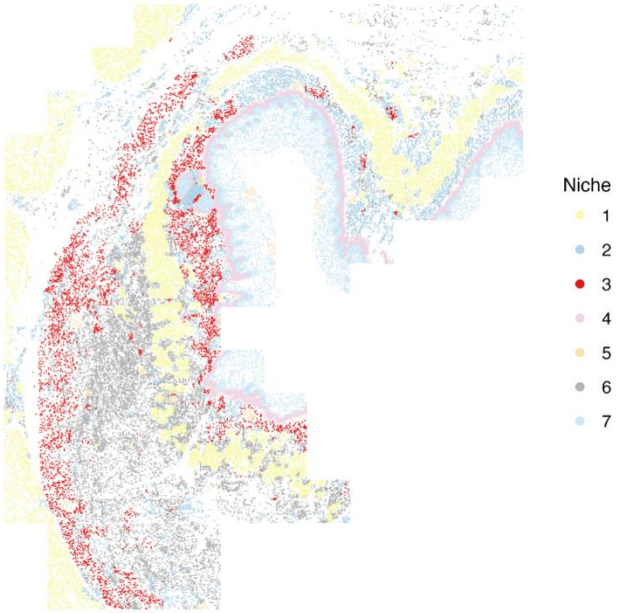

OAC4R

Niche 1
Endo/mural

Niche 2
Univ. fib, Trans. fib, Stress CAF, M1 Mac, M2 Mac, Mono, DC, Gran

Niche 3
Cancer, Quiescent fib 2, Stress CAF, MyoCAF, DesmoCAF, M2 Mac, DC

Niche 4
Basal squam. epi, Cycling basal squam. epi, Diff. squam. epi

Niche 5
M2 Mac, Diff. squam. epi, Barrett's-like epi

Niche 6
Cancer, Quiescent fib 1, T cell, Treg, NK cell, B cell, Plasma, Gran

Niche 7
Cycling basal squam. epi, Diff. squam. epi

Supplementary Figure S6 Spatial localisation and composition of multicellular niches. Spatial maps of unsupervised niche assignments in representative resection samples from **a)** OAC1, **b)** OAC2, and **c)** OAC4. Cells are coloured by niche identity. Summary boxes indicate the dominant or enriched cell types contributing to each niche, including cancer-enriched, fibroblast/CAF-enriched, immune-enriched, epithelial-enriched, and mixed stromal–immune neighbourhoods.

OAC1

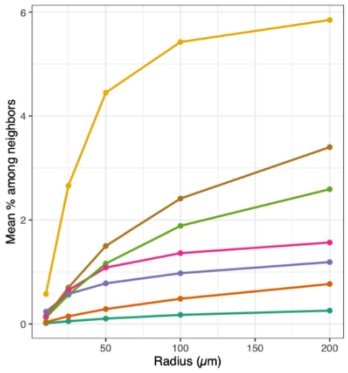

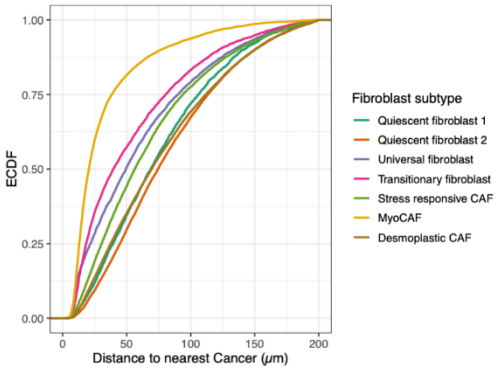

OAC2

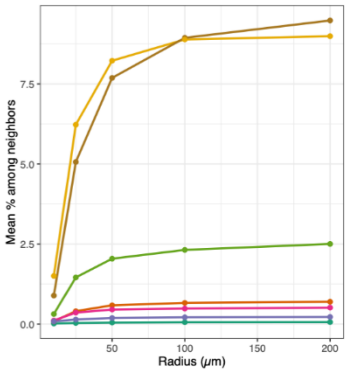

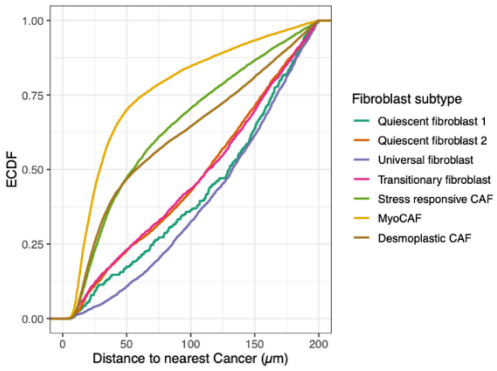

OAC3

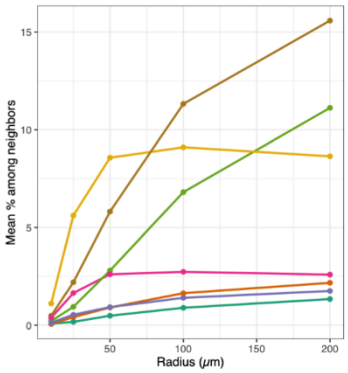

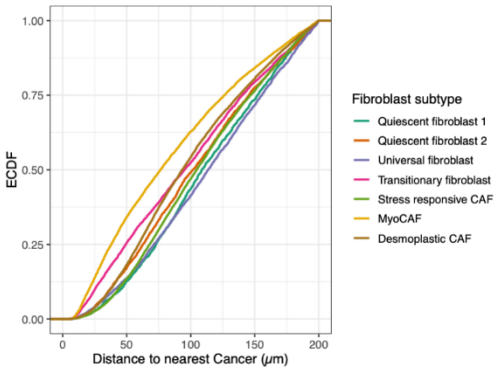

OAC4

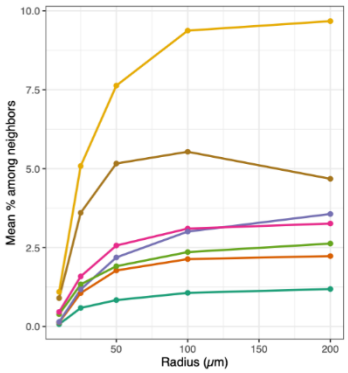

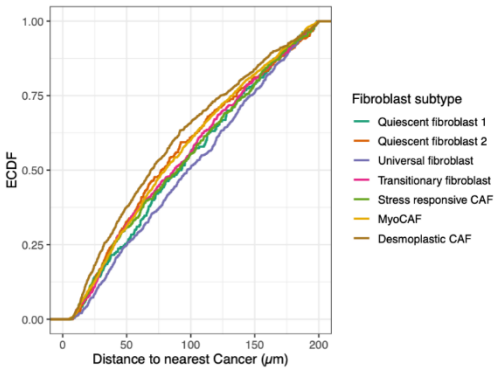

OAC5

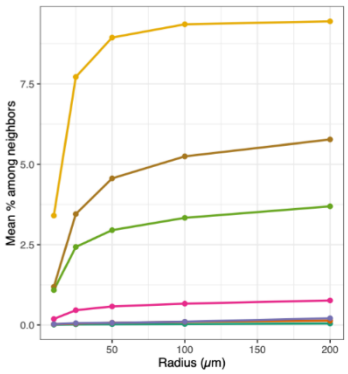

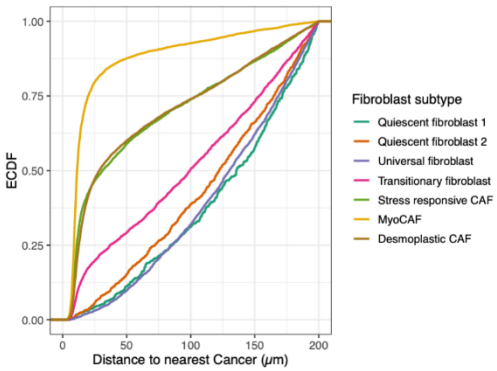

Supplementary Figure S7 Cancer-centred spatial organisation of fibroblast subtypes. For each resection sample, left panels show the mean percentage of neighbouring cells assigned to each fibroblast subtype at increasing distances from cancer cells. Right panels show empirical cumulative distribution functions for the distance from each fibroblast subtype to the nearest cancer cell. Curves shifted upward at shorter distances indicate closer spatial proximity to malignant epithelium.

a

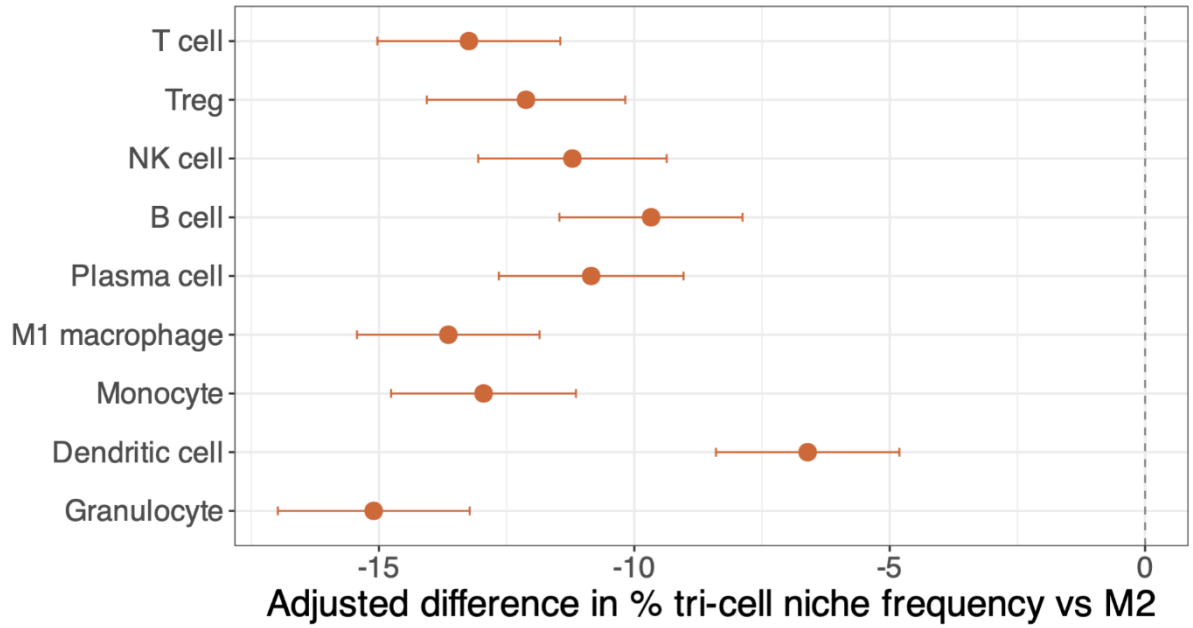
T cell
Treg
NK cell
B cell
Plasma cell
M1 macrophage
Monocyte
Dendritic cell
Granulocyte
-15
-10
-5
0
Adjusted difference in % tri-cell niche frequency vs M2

b

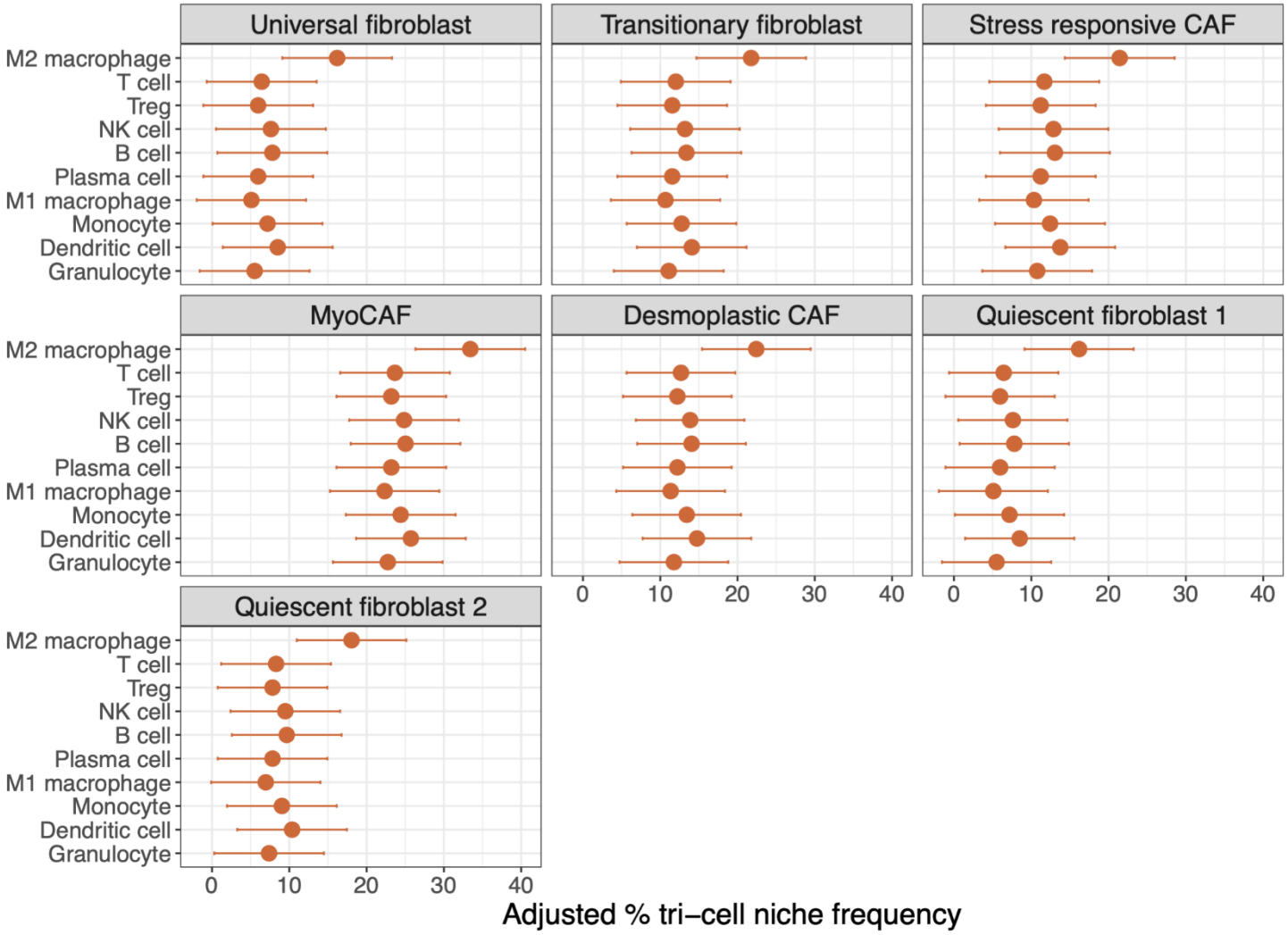
Universal fibroblast
Transitionary fibroblast
Stress responsive CAF
MyoCAF
Desmoplastic CAF
Quiescent fibroblast 1
Quiescent fibroblast 2
M2 macrophage
T cell
Treg
NK cell
B cell
Plasma cell
M1 macrophage
Monocyte
Dendritic cell
Granulocyte
0
10
20
30
40
Adjusted % tri−cell niche frequency

Supplementary Figure S8 Abundance-adjusted modelling of fibroblast–immune tri-cell niches around cancer cells. a) Model-estimated differences in the percentage of cancer cells occupying MyoCAF-containing tri-cell niches with each immune subtype, relative to M2 macrophages. Negative values indicate lower adjusted niche frequency compared with M2 macrophage-containing niches. **b)** Adjusted tri-cell niche frequencies for combinations of fibroblast and immune subtypes. Points and horizontal intervals show model-estimated frequencies and uncertainty intervals after adjustment for sample-level cell-type abundance and patient structure.

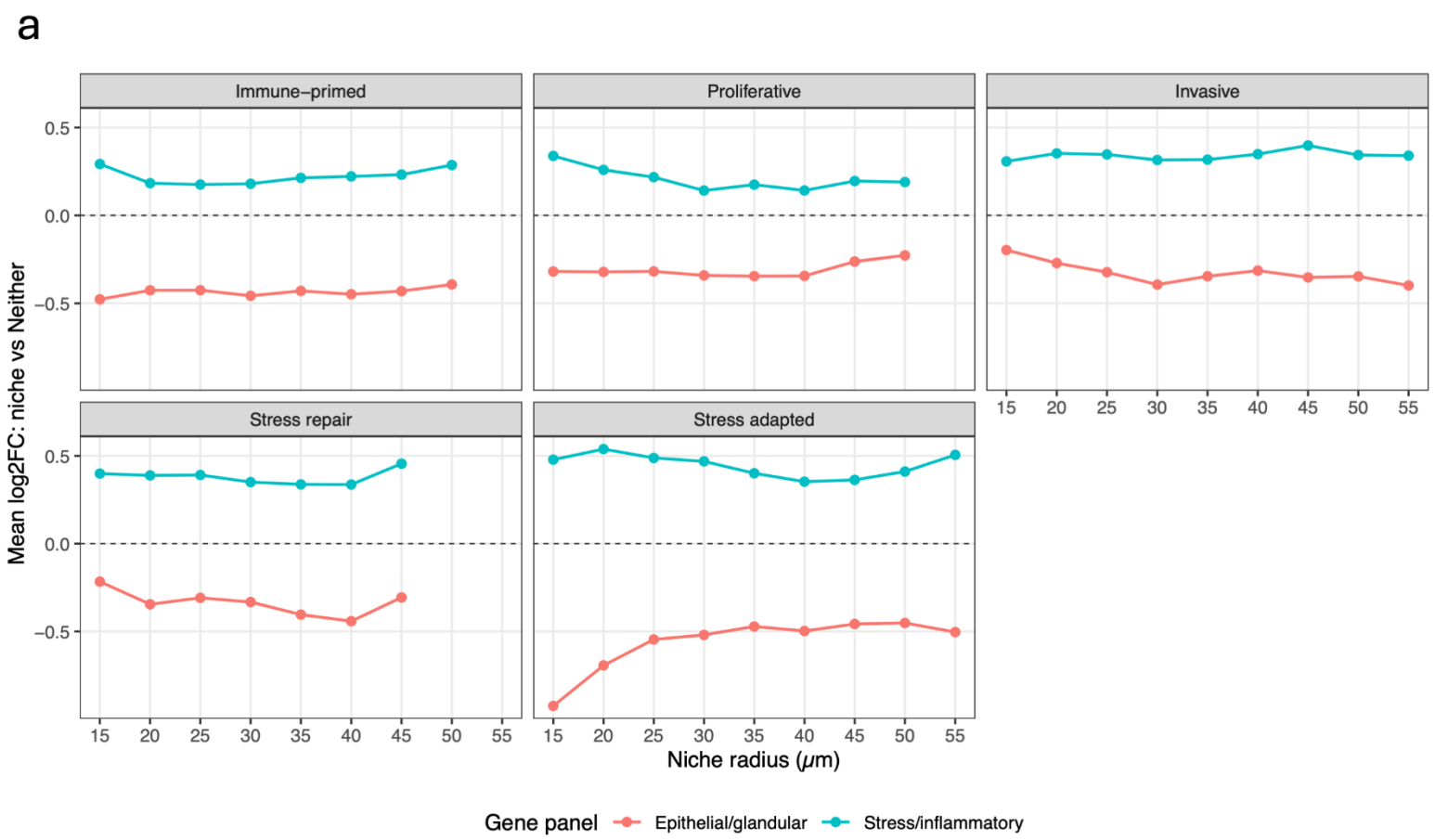
a
Immune–primed
Proliferative
Invasive
Stress repair
Stress adapted
Mean log2FC: niche vs Neither
0.5
0.0
−0.5
15
20
25
30
35
40
45
50
55
Niche radius (μm)
Gene panel
Epithelial/glandular
Stress/inflammatory

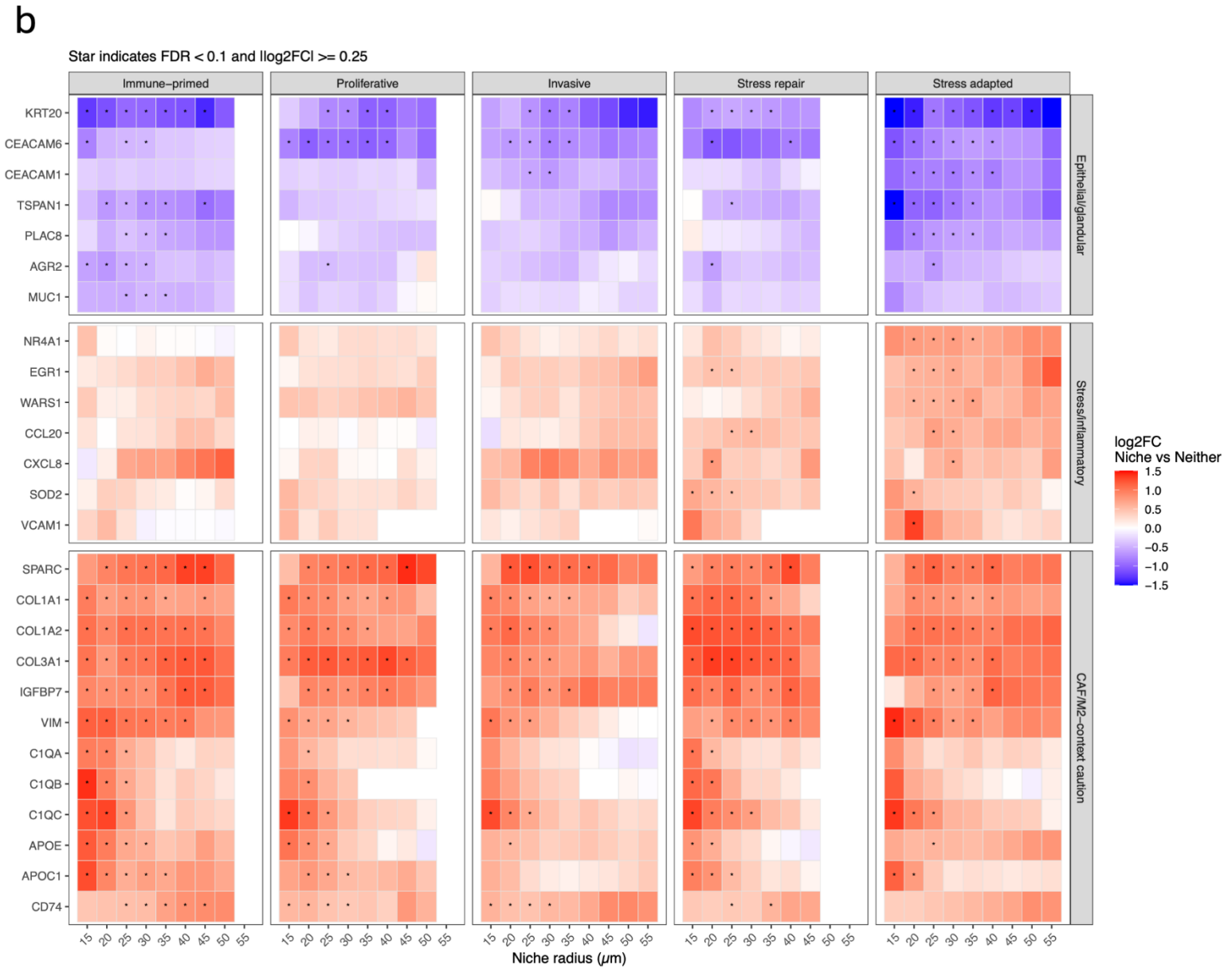
b
Star indicates FDR < 0.1 and |log2FC| >= 0.25
Immune–primed
Proliferative
Invasive
Stress repair
Stress adapted
KRT20
CEACAM6
CEACAM1
TSPAN1
PLAC8
AGR2
MUC1
NR4A1
EGR1
WARS1
CCL20
CXCL8
SOD2
VCAM1
SPARC
COL1A1
COL1A2
COL3A1
IGFBP7
VIM
C1QA
C1QB
C1QC
APOE
APOC1
CD74
Epithelial/glandular
Stress/inflammatory
CAF/M2–context caution
log2FC
Niche vs Neither
1.5
1.0
0.5
0.0
−0.5
−1.0
−1.5
15
20
25
30
35
40
45
50
55
Niche radius (μm)

Supplementary Figure S9 Radius sensitivity of MyoCAF–M2 macrophage niche-associated cancer-cell transcriptional changes. a) Mean log2 fold change of epithelial/glandular and stress/inflammatory gene categories in cancer cells located in a MyoCAF–M2 macrophage niche versus cancer cells lacking nearby MyoCAFs and M2 macrophages, across niche radii. Results are shown separately for each malignant cNMF programme. **b)** Heatmap of niche-associated log2 fold changes for selected epithelial/glandular, stress/inflammatory, and CAF/M2-conditioned genes across neighbourhood radii and tumour programmes. Markers indicate genes meeting the exploratory significance threshold of FDR < 0.1 and absolute log2 fold change ≥ 0.25.